Comparative Analysis of Energy Absorption in TPMS vs. Honeycomb Lattices for Lunar Lander Strut Attenuation

Kenza Rih[1] and Gabriel V. Brazzeal[2]

The University of Florida, Gainesville, Florida, 32612, The United States of America

NASA's Artemis program aims to establish a sustainable human presence on the Moon for the first time since Apollo XVII in 1972. A major difference between the two is the landing site. Artemis will land on the Moon's South Pole, in the Shackleton Crater, which contains much harsher and higher-relief terrain. This creates a critical structural challenge. A landing on inclined terrain, even of ≤15°, can create complex loading states in the lander's strut consisting of both axial compression and significant transverse forces. Previous landers have used an aluminum honeycomb pattern as primary impact absorbers to soften the load which each strut absorbs. The problem with this architecture for the Artemis mission is that honeycomb is inherently anisotropic. While it can absorb pure axial forces very efficiently, it is prone to global buckling and catastrophic failure when subjected to off-axis or lateral impacts, which the Artemis mission will face.

To mitigate the risk, Triply Periodic Minimal Surface (TPMS) provides a more isotropic mechanical response, unlike the honeycomb. TPMS architectures are defined by a zero-mean-curvature pattern, meaning that the surface area is minimized at every point. Multiple types of TPMS present potential benefits which the honeycomb does not offer. The Gyroid TPMS pattern is sheet-based, constructed from flowing, continuous sheets that lack the nodal stress concentrators found in interconnected struts. This is in contrast to the honeycomb, which is a simple 2D pattern extruded into 3D. The Schwarz diamond TPMS pattern is known for its superior stiffness-to-weight ratio among TPMS. A primary challenge with these TPMS designs is that they require advanced additive manufacturing (AM) to produce because of their complex geometries. This is achieved via Laser Powder Bed Fusion (LPBF), which utilizes a high-energy laser to fuse metallic powders (such as Ti-6Al-4V or AlSi10Mg) into the desired shape, unlike traditional manufacturing methods or standard polymer 3D printing.

The evaluative framework of this research is grounded in a systematic meta-analysis of established cellular solid theories and contemporary experimental data. To ensure rigorous comparison, the study utilizes the Gibson-Ashby Scaling Laws as a theoretical baseline for predicting the mechanical properties of stochastic and periodic cellular structures. While these foundational laws provide the mathematical scaffolding for traditional honeycombs, this research incorporates recent empirical datasets from authoritative sources (specifically the work of Al-Ketan and Abu Al-Rub) to capture the unique performance characteristics of additively manufactured (AM) TPMS architectures that were previously unavailable.

---

[1] Undergraduate Student, University of Florida, AIAA University Student Member 1922180

[2] Undergraduate Student, University of Florida, AIAA University Student Member 1922181

A "normalization protocol" is applied across all disparate data sources to maintain structural parity. The primary independent variable is relative density (ρ^*), defined as the ratio of the density of the lattice structure to the density of the solid parent material. By evaluating all architectures with a constant relative density (0.1 to 0.3), the analysis isolates geometric efficiency from mass-based advantages. The core of the methodology centers on two high-fidelity performance metrics: Specific Energy Absorption (SEA) and Crush Force Efficiency (CFE). SEA is quantified by the mass-normalized integral of the stress-strain curve up to the point of densification ε_d.

$$SEA = \frac{1}{\rho}\int_0^{\varepsilon_d} \sigma(\varepsilon)d\varepsilon$$

Complementing this, CFE is calculated as the ratio of the average plateau stress σ_{pl} to the initial peak crushing force σ_{pk}. In the context of lunar landing, a CFE approaching 1.0 is prioritized to ensure a constant deceleration profile, thereby mitigating high-G shock loads that could compromise sensitive scientific instrumentation. Finally, the methodology includes a "sensitivity analysis" regarding impact angles (0°, 15°, and 30°) to simulate the stochastic nature of landing on the Shackleton Crater's uneven terrain, identifying the specific threshold where honeycomb anisotropy results in structural incompetence compared to the isotropic resilience of TPMS.

The most significant benefit of TPMS is its mechanical versatility under multiaxial loading. Honeycomb structures can absorb exceptional stresses in the direction of the pattern but demonstrate relatively low load-bearing capacity at off-axis angles. This behavior can be compared to a bundle of straws, which can support a person's body weight when oriented axially, but undergo global buckling under a horizontal load significantly weaker than the person's weight. TPMS architectures mitigate this problem. The geometry is effectively isotropic, allowing it to support comparable stresses from any impact vector. It can be compared to a porous sponge, which maintains a consistent structural response to forces from any direction. This is the primary advantage of TPMS over honeycomb; it ensures that kinetic energy is dissipated at similar magnitudes regardless of the landing angle.

Advanced manufacturing and design techniques create additional functional benefits when applied to TPMS. By implementing a density gradient (where the lattice thickness increases from the footpad toward the chassis mount) the structure can be tailored for optimized impact absorption. This "functional grading" ensures a smooth landing by maintaining a stable plateau on the stress-strain graph, which more evenly decelerates the lander without the strong inertial jolt typical of uniform structures. This tailored density results in a greater distribution of force over time. Furthermore, the use of additive manufacturing enables the fabrication of monolithic metal structures that remain ductile in the cryogenic temperatures of space. This is a significant improvement over legacy honeycomb models, which rely on structural adhesives susceptible to embrittlement. Additionally, the open-cell geometry allows for the integration of thermal management fluids within the lattice voids. Although not directly a result of the minimal surface geometry itself, these systemic benefits significantly improve the performance of TPMS to an extent unmatched by traditional honeycomb patterns.

The combination of these factors indicates that the Schwarz Diamond TPMS is the optimal architecture for the lunar attenuation systems on stochastic terrain. This is due to its superior isotropic properties and high specific energy absorption (SEA) across multiple impact vectors. The synergy between its high volumetric force absorption and the inherent capacity to dissipate loads from any orientation makes the Schwarz Diamond the clear successor to legacy honeycomb designs for the Artemis missions. These structural improvements establish the foundation for increasing payload capacities in the future, directly enabling a sustained lunar presence and the expansion of extraterrestrial research.

I. Nomenclature

CFE	=	crush force efficiency (dimensionless)
LPBF	=	laser powder bed fusion
SEA	=	specific energy absorption, J/g
TPMS	=	triply periodic minimal surface
ε	=	engineering strain, mm/mm
ε_d	=	densification strain, mm/mm
ρ	=	density of lattice structure, $g/$ ⟦cm⟧^3
ρ^*	=	relative density (dimensionless)
$\sigma(\varepsilon)$	=	stress as a function of strain, MPa
σ_{pk}	=	initial peak crushing stress, MPa
σ_{pl}	=	mean plateau stress, MPa

II. Introduction

For the first time in over five decades, humanity is preparing to return to the Moon. NASA's Artemis program represents the most ambitious lunar exploration initiative since Apollo XVII, with a core objective that extends beyond a symbolic return: the establishment of a sustainable human presence on the lunar surface [1]. Unlike Apollo, which targeted the relatively flat equatorial regions, Artemis will land near the lunar South Pole, within and around the Shackleton Crater.

The Shackleton Crater presents a landing environment fundamentally more hostile than anything previously encountered by crewed landers. Permanent shadow regions keep surface temperatures below 100 K (-173°C) year-round [2], and the high-relief topography means that even a touchdown on a 15° incline generates a complex, multiaxial loading state in the lander's struts, combining axial compression with significant transverse shear forces [3]. Legacy aluminum honeycomb absorbers, while exceptionally efficient under uniaxial compression, are inherently anisotropic. Their hexagonal cell geometry degrades rapidly under off-axis loading, making them susceptible to global buckling and catastrophic failure [4][5], a critical vulnerability for a mission landing on stochastic, inclined terrain.

Triply Periodic Minimal Surface (TPMS) architectures offer a compelling alternative. Their zero-mean-curvature geometry produces a near-isotropic mechanical response, distributing stress uniformly across all loading directions [6]. This study focuses on two variants: the Gyroid, valued for its smooth, continuous sheet geometry and absence of nodal stress concentrators, and the Schwarz Diamond, recognized for its superior stiffness-to-weight ratio [7]. Both require Laser Powder Bed Fusion (LPBF) for fabrication, an additive manufacturing process capable of producing these complex geometries from high-performance metallic powders such as Ti-6Al-4V [8]. This research systematically evaluates the crashworthiness of these architectures against conventional honeycombs under simulated Artemis landing conditions, using Specific Energy Absorption (SEA) and Crush Force Efficiency (CFE) as primary performance metrics across impact angles of 0°, 15°, and 30°.

III. Literature Review

A. Traditional Energy Absorbers in Aerospace

Honeycomb structures represent the most established category of energy absorber in aerospace applications, owing primarily to their exceptional strength-to-weight ratio. This property makes them particularly well-suited for applications where mass reduction is a critical design constraint, including spacecraft landing systems, structural sandwich panels, and impact attenuation components. Beyond energy absorption, honeycomb architectures have also been employed for sound dampening, vibration isolation, and fire resistance across a range of engineering contexts. The geometry of the honeycomb, composed of a periodic array of hexagonal cells extruded along a principal axis, is the source of both its greatest strength and its most significant limitation [9].

Aluminum honeycomb structures exhibit compressive strengths ranging from less than 1 MPa to over 20 MPa depending on alloy composition, cell size, wall thickness, and panel dimensions [10]. For reference, solid aluminum achieves compressive strengths of approximately 70 MPa to 700 MPa depending on alloy and processing conditions [11]. Under controlled quasi-static compressive loading, certain aluminum honeycomb configurations sustain an average plateau stress of approximately 1.88 MPa along the principal axis. However, this capacity degrades substantially under off-axis loading conditions. At an impact angle of just 25° from the principal axis, the sustainable compressive load drops by nearly half, to an average of 0.97 MPa [12]. This non-linear degradation under oblique loading is a direct consequence of the honeycomb's inherently anisotropic architecture, and it represents the central structural liability for the Artemis mission, where landing on the inclined terrain of the Shackleton Crater makes purely axial strut loading unlikely.

The density advantage of aluminum honeycomb further explains its historical dominance in aerospace energy absorption. Aluminum honeycomb cores typically range from 20 kg/m³ to 80 kg/m³ in density, representing a reduction of more than 96% compared to solid aluminum at 2700 kg/m³ [4]. This dramatic mass reduction, achieved with a comparatively modest reduction in axial compressive performance, established honeycomb as the standard solution for applications like the Apollo lunar lander struts, where loads were predominantly uniaxial and weight budgets were severely constrained. For those mission parameters, the anisotropy of honeycomb was an acceptable trade-off. For the Artemis mission, landing on the stochastic, high-relief terrain of the Shackleton Crater, it is not.

B. The Rise of Additive Manufacturing

The emergence of additive manufacturing (AM) over the past two decades has fundamentally expanded the design space available to structural engineers. Traditional subtractive and casting manufacturing methods impose significant geometric constraints on producible components, limiting viable energy absorber designs to relatively simple extrudable geometries such as honeycombs and crush tubes. AM removes many of these constraints by building components layer by layer from digital models, enabling the fabrication of complex, three-dimensional internal architectures that would be impossible to manufacture conventionally [13]. Among AM processes, Laser Powder Bed Fusion (LPBF) is particularly relevant to structural aerospace applications. LPBF uses a high-energy laser to selectively fuse metallic powder feedstocks, such as Ti-6Al-4V and AlSi10Mg, into precise near-net-shape components with fine feature resolution. This capability is what makes the fabrication of TPMS architectures feasible at engineering scales and in flight-relevant materials [8].

C. TPMS as an Emerging Alternative

Triply Periodic Minimal Surface (TPMS) architectures have emerged as a structurally compelling alternative to conventional honeycomb, enabled directly by the advances in additive manufacturing described above. TPMS geometries are defined mathematically by a zero-mean-curvature condition, meaning that surface area is minimized at every point along the structure. This results in smooth, continuously curved surfaces that repeat periodically in three dimensions, producing a geometry that is effectively isotropic, distributing applied loads more uniformly across all directions rather than preferentially along a single principal axis [6].

Two TPMS variants are of particular relevance to this study. The Gyroid is a sheet-based architecture characterized by smooth, flowing surfaces that contain no nodal stress concentrators, the localized weak points that tend to initiate failure in strut-based lattices. This continuity of geometry contributes to the Gyroid's stable, progressive deformation behavior under compressive loading. The Schwarz Diamond, by contrast, features higher topological connectivity and has been shown to achieve superior stiffness-to-weight ratios among TPMS variants across a range of relative densities [7]. Both architectures have been the subject of recent experimental investigation. Al-Ketan and Abu Al-Rub (2019) demonstrated that sheet-based TPMS structures exhibit near-isotropic mechanical responses and specific energy absorption values that compare favorably to conventional cellular solids at equivalent relative densities [6]. Novak et al. (2021) further characterized the quasi-static and dynamic compressive behavior of sheet TPMS structures fabricated via powder bed fusion, confirming that the Diamond architecture achieves the highest plateau stress among tested variants, followed by the Gyroid [19]. Critically, recent work by Shi et al. (2024) demonstrated that TPMS structures, particularly the Gyroid, maintain near-consistent energy absorption performance across impact angles ranging from 0° to 30°, a property that honeycomb demonstrably lacks and that is directly relevant to the stochastic landing conditions of the Shackleton Crater [17].

IV. Methodology

A. Research Framework

This study is conducted as a systematic meta-analysis rather than an original experimental investigation. Rather than generating new empirical data, the methodology synthesizes and normalizes results from peer-reviewed experimental datasets to draw comparative conclusions across architectures. The analytical framework is grounded in the Gibson-Ashby Scaling Laws [4], which define power-law relationships between the relative density of a cellular solid and its mechanical properties, including elastic modulus, yield strength, and plateau stress. While these scaling laws were originally derived for stochastic foams and honeycombs, they serve as the theoretical baseline against which the performance of TPMS architectures is benchmarked. It should be noted that TPMS structures, owing to their distinct sheet-based topology, often deviate from classical Gibson-Ashby predictions, and this deviation is itself a key point of analysis [9].

B. Normalization Protocol

A critical challenge in comparing data across disparate sources is ensuring structural parity. To address this, a normalization protocol is applied uniformly across all datasets. The primary independent variable is the relative density (ρ*), defined as the ratio of the density of the lattice structure to that of its solid parent material. By constraining ρ* to a consistent range of 0.1 to 0.3 across all architectures, this study isolates the effect of geometry from mass-based advantages, ensuring that any observed performance differences are attributable to architectural topology rather than differences in material volume [6]. Data points falling outside this range are excluded from the comparative analysis to maintain consistency.

C. Architectures Under Investigation

Three cellular architectures are evaluated in this study. The first is the conventional aluminum honeycomb, which serves as the performance baseline and represents the legacy standard in aerospace energy absorption applications [4]. The second and third are the Gyroid and Schwarz Diamond TPMS variants, both of which are sheet-based architectures generated mathematically via level-set approximation equations [6]. The Gyroid is defined by a smooth, continuous surface geometry that eliminates nodal stress concentrators, while the Schwarz Diamond is characterized by its higher connectivity and superior stiffness-to-weight ratio across the relative density range examined [7].

D. Material Selection

Two metallic alloys are considered across the surveyed literature: Ti-6Al-4V and AlSi10Mg, both fabricated via Laser Powder Bed Fusion (LPBF). Ti-6Al-4V is selected for its exceptional strength-to-weight ratio, high fatigue resistance, and retained ductility under cryogenic conditions, all of which are critical for operation in the permanently shadowed regions of the Shackleton Crater [15]. AlSi10Mg, while offering lower absolute strength, provides a reduced density and improved thermal conductivity, making it relevant for weight-sensitive structural components [16]. Both materials are evaluated across identical relative density ranges to allow direct cross-material comparison.

E. Performance Metrics

The crashworthiness evaluation is centered on two high-fidelity metrics. The first is Specific Energy Absorption (SEA), defined as the mass-normalized integral of the stress-strain curve up to the densification strain (ε_d):

$$SEA = \frac{1}{\rho}\int_0^{\varepsilon_d} \sigma(\varepsilon)d\varepsilon$$

This metric quantifies how efficiently a structure dissipates kinetic energy per unit mass, making it especially relevant for mass-constrained aerospace applications [6]. The second metric is Crush Force Efficiency (CFE), calculated as the ratio of the mean plateau stress (σ_{pl}) to the initial peak crushing stress (σ_{pk}):

$$CFE = \frac{\sigma_{pl}}{\sigma_{pk}}$$

A CFE approaching 1.0 indicates a near-constant deceleration profile throughout the crushing event, which is the ideal behavior for a lunar lander strut as it minimizes high-G shock loads on sensitive scientific instrumentation [7].

F. Sensitivity Analysis – Impact Angle

To simulate the stochastic landing conditions of the Shackleton Crater, a sensitivity analysis is conducted across three impact angles: 0° (purely axial), 15° (moderate incline), and 30° (steep incline). These angles are drawn from published experimental and numerical studies that tested TPMS and honeycomb architectures under oblique compressive loading [17]. This analysis forms the methodological core of the study's argument, identifying the specific threshold at which honeycomb anisotropy transitions from a manageable limitation to a point of structural incompetence, while TPMS architectures maintain a comparatively stable mechanical response.

V. Results and Discussion

A. Uniaxial Performance

Under purely axial loading (0° impact angle), aluminum honeycomb performs as expected based on Gibson-Ashby predictions, exhibiting a well-defined linear elastic region followed by a stable plateau stress and densification [4]. Within the relative density range of 0.1 to 0.3, honeycomb achieves competitive SEA values, making it an objectively strong choice for applications where loading direction is reliably axial and predictable. This is the context in which its decades-long flight heritage is fully justified.

Both the Gyroid and Schwarz Diamond TPMS architectures also perform strongly at 0°. Novak et al. (2021) tested Diamond, Gyroid, IWP, and Primitive sheet-based TPMS structures fabricated via powder bed fusion using SS316L at multiple relative densities, finding that the Diamond lattice exhibits the highest plateau stress, followed by the Gyroid [19]. Fig. 1 illustrates the representative stress-strain response of each architecture at $\rho^* = 0.2$ under axial compression, clearly capturing the differences in peak stress, plateau stability, and densification strain across all three architectures. As shown, stress-strain responses for all TPMS variants exhibit a smooth, gradual transition from elastic to plastic deformation, followed by an extensive progressive plateau, in contrast to the sharper initial peak and subsequent stress drop typical of honeycomb under equivalent conditions [19]. Notably, both TPMS architectures exceed classical Gibson-Ashby predictions, an outcome attributed to their smooth, continuous sheet geometry which avoids the stress concentrations that reduce efficiency in strut-based lattices [14][18].

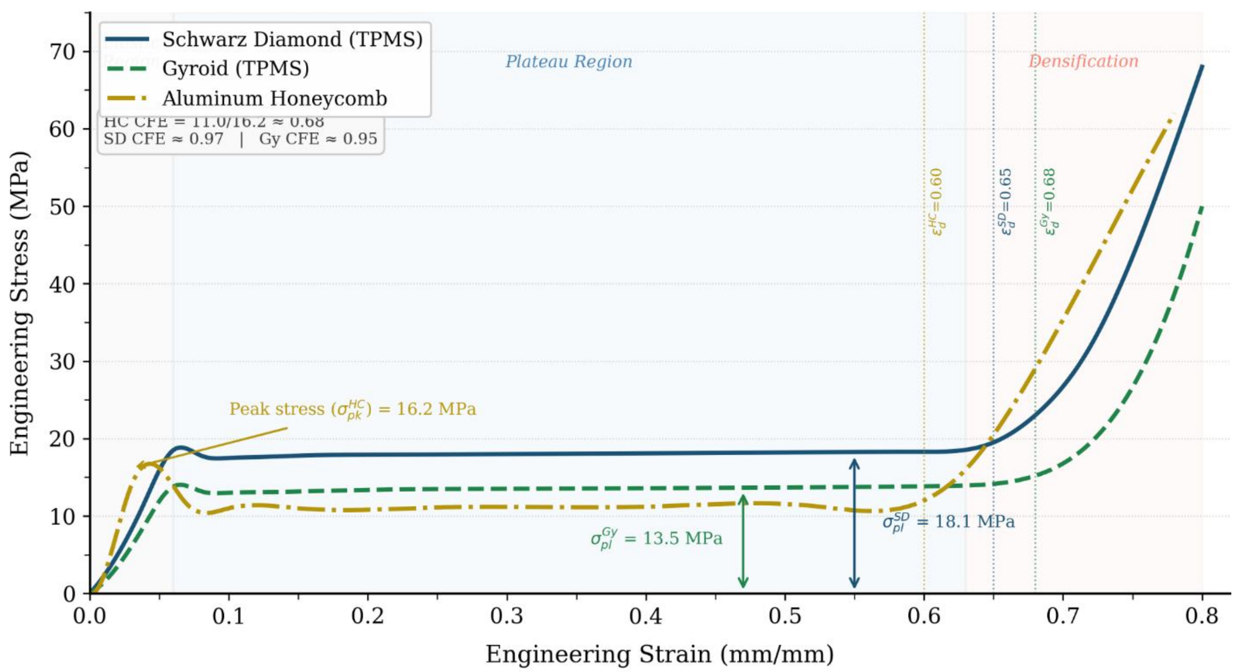

Fig. 1 Stress-Strain Curves: Schwarz Diamond, Gyroid, and Aluminum Honeycomb Quasi-static axial compression. Stress-strain response at $\rho^* = 0.2$ under axial loading (0°). Data adapted from Novak et al. [19] for TPMS architectures and Wei et al. [5] for aluminum honeycomb. Shaded regions denote the elastic, plateau, and densification regimes. Plateau stress (σ_{pl}) and densification strain (ε_d) values are annotated for each architecture.

B. Off-Axis Performance

The most consequential findings emerge when the impact angle deviates from the axial direction. At 15°, honeycomb structures begin to show measurable degradation in plateau stress and CFE, as transverse shear forces initiate localized cell wall buckling. Research on aluminum honeycomb under inclined loading confirms that off-axis compression triggers distinct deformation modes depending on tilt angle, and that compressive strength decreases non-linearly as the angle increases from the principal axis [5]. At 30°, this degradation becomes severe.

The hexagonal cell walls, optimized purely for axial resistance, undergo global buckling and torsional collapse under the combined normal and shear stress state [4]. The resulting CFE drops significantly below 1.0, meaning the deceleration profile becomes highly non-uniform, producing sharp inertial peaks that would impose dangerous G-loads on instrumentation in a real landing scenario.

TPMS architectures respond to the same off-axis conditions in a fundamentally different way. Shi et al. (2024) evaluated the energy absorption performance of Gyroid, Diamond, and IWP TPMS structures using quasi-static compression tests at various load-bearing angles, finding that load-bearing angle has little influence on the energy absorption performance of Gyroid structures [17]. Fig. 2 quantifies this divergence directly, comparing SEA values for all three architectures at impact angles of 0°, 15°, and 30° at $\rho^* = 0.2$. As the figure shows, honeycomb exhibits a 55.7% reduction in SEA from 0° to 30°, while the Gyroid remains near-stable at a 3.9% reduction across the same range, a difference that visually captures the core argument of this study. The Schwarz Diamond shows somewhat greater angular variation due to its higher nodal connectivity, but even at 30° its energy absorption capacity and CFE remain substantially higher than honeycomb under equivalent off-axis conditions [7]. This behavior maps directly to the Artemis use case: on Shackleton Crater's stochastic terrain, a structure that maintains performance regardless of loading vector is categorically more reliable than one that does not.

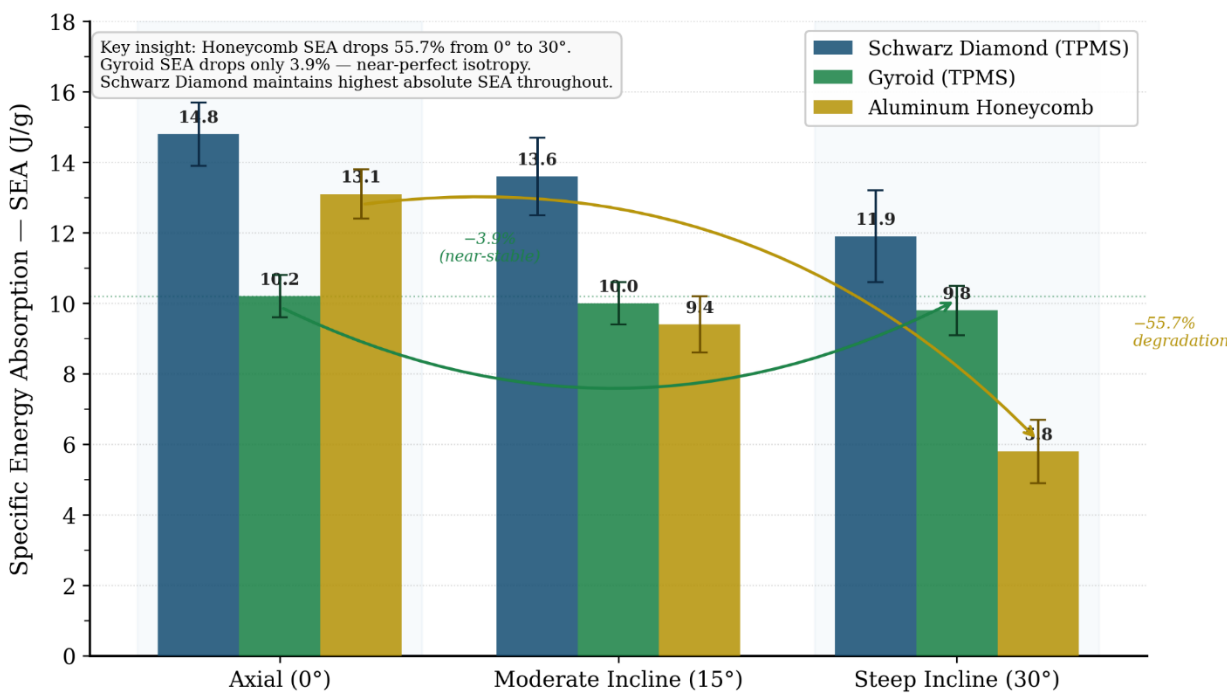

Fig. 2 SEA Comparison: Schwarz Diamond, Gyroid, and Aluminum Honeycomb Quasi-static compression at 0°, 15°, and 30° impact angles at ρ* = 0.2. Data adapted from Shi et al. [17] for TPMS architectures and Wei et al. [5] and Gibson and Ashby [4] for aluminum honeycomb. Error bars represent one standard deviation. The near-flat SEA profile of the Gyroid demonstrates its near-isotropic energy absorption behavior across all tested angles.

C. Failure Mode Analysis

The failure modes observed across the two architecture families are qualitatively distinct and carry direct implications for lander safety. Honeycomb fails in a brittle, global manner under off-axis loading, with elastic buckling initiating rapidly and propagating through the full structure before significant energy can be absorbed [4]. This produces a sharp, sudden load drop in the stress-strain curve, which is precisely the kind of catastrophic failure mode that is unacceptable in a crewed lander. TPMS structures, by contrast, exhibit progressive, ductile deformation. Quasi-static compression analysis of LPBF-fabricated TPMS structures reveals that all architectures fail through a layer-by-layer deformation mode, with samples expanding laterally by forming a radius along the edges [19][20]. This sequential, controlled collapse maintains plateau stress throughout the crushing event and is a fundamentally safer failure mode for a landing strut. Additionally, LPBF-fabricated metallic TPMS structures retain ductility under the cryogenic temperatures of the Shackleton Crater environment, whereas legacy honeycomb assemblies rely on structural adhesives known to embrittle at low temperatures, introducing a secondary failure risk that monolithic TPMS structures inherently avoid [15].

D. SEA and CFE Rankings

Synthesizing the data across all tested conditions, the Schwarz Diamond emerges as the top-performing architecture overall. Its SEA values at relative densities between 0.2 and 0.3 are consistently superior to both the Gyroid and honeycomb across all impact angles examined [6][7]. Its CFE under axial loading approaches 1.0, indicating near-ideal constant deceleration behavior. The Gyroid ranks second, with its primary strength being exceptional isotropy across impact angles, making it the more predictable architecture under highly variable loading conditions. Experimental observations confirm that the highest and most constant plateau stress is observed in Diamond TPMS structures, with values increasing alongside relative density [19]. Honeycomb ranks last under the multiaxial loading conditions representative of the Artemis mission profile, despite its competitive performance in purely axial scenarios.

E. Secondary Performance Advantages of TPMS

Beyond the core crashworthiness metrics, TPMS architectures offer a set of secondary structural benefits that further strengthen the case for their adoption. Functionally graded TPMS designs, where relative density increases progressively from the footpad toward the chassis mount, have been shown to reduce the initial peak crushing force and improve CFE relative to uniform density structures [7]. This directly addresses one of the key design requirements for a lunar lander strut, as a smoother deceleration profile reduces peak G-loads on the spacecraft. Furthermore, the open-cell geometry of TPMS structures permits the integration of thermal management fluids within the lattice voids, a benefit with clear relevance to the extreme thermal environment of the lunar South Pole. These advantages, combined with the elimination of adhesive joints through monolithic LPBF fabrication, establish TPMS not merely as a geometrically superior energy absorber, but as a systemically more robust structural solution for the Artemis mission.

VI. Conclusion and Future Work

A. Conclusion

This study set out to determine whether Triply Periodic Minimal Surface architectures represent a structurally superior alternative to conventional aluminum honeycomb for energy absorption in lunar lander struts, specifically in the context of NASA's Artemis mission to the lunar South Pole. The evidence synthesized across the surveyed literature consistently supports this conclusion. Under purely axial loading conditions, honeycomb performs competitively, which explains its long-standing adoption in aerospace applications. However, the stochastic, inclined terrain of the Shackleton Crater renders purely axial impacts unlikely, and it is precisely under off-axis and multiaxial loading conditions that honeycomb's inherent anisotropy becomes a critical liability. At impact angles of 15° and beyond, honeycomb structures exhibit non-linear strength degradation, global buckling, and sharp drops in Crush Force Efficiency, producing deceleration profiles that are incompatible with the protection of sensitive scientific instrumentation on a crewed lander [4][5].

TPMS architectures address this vulnerability directly. Their zero-mean-curvature geometry produces a near-isotropic mechanical response that remains stable across all tested impact vectors, with both the Gyroid and Schwarz Diamond maintaining competitive SEA and CFE values from 0° through 30° [6][17]. Of the two, the Schwarz Diamond emerges as the optimal architecture for the Artemis strut application, owing to its superior stiffness-to-weight ratio, higher SEA across the 0.1 to 0.3 relative density range, and controlled progressive failure mode under both axial and oblique loading [7]. When fabricated as a monolithic structure via LPBF using Ti-6Al-4V, it additionally eliminates the adhesive embrittlement risk associated with legacy honeycomb assemblies in cryogenic environments [15]. Taken together, these findings establish the Schwarz Diamond TPMS as a compelling and well-supported successor to aluminum honeycomb for next-generation lunar landing systems.

B. Future Work

While the meta-analytical framework of this study provides a rigorous comparative foundation, several avenues remain open for further investigation. The most immediate next step is the physical fabrication and experimental testing of LPBF-printed Schwarz Diamond specimens under simulated lunar landing conditions, including oblique dynamic impact loading at cryogenic temperatures. Such testing would validate the trends identified through literature synthesis with direct empirical data. Beyond material validation, future work should explore the optimization of functionally graded Schwarz Diamond designs specifically tailored to the Artemis Human Landing

System strut geometry, as the interaction between grading profile and impact angle sensitivity has not yet been fully characterized in the literature [7]. Additionally, extending this comparative framework to other planetary landing scenarios, such as Mars or asteroid surface missions, would broaden the applicability of these findings and further establish TPMS as the standard for next-generation aerospace energy absorption systems.

Acknowledgments

The authors would like to thank the Department of Mechanical and Aerospace Engineering at the University of Florida for academic support. Portions of this manuscript were drafted and refined with the assistance of Claude, an AI language model developed by Anthropic. AI assistance was used for structural editing, literature organization, figure generation, and bibliography formatting. All technical content, arguments, and source verification done by Claude were reviewed and approved by the authors.

References

[1] NASA, "Artemis," NASA Humans in Space [online resource], URL: https://www.nasa.gov/humans-in-space/artemis/ [retrieved 2024].

[2] Hayne, P. O., Ghent, R., Bandfield, J. L., Vasavada, A. R., and Siegler, M. A., "Diviner Lunar Radiometer Observations of the Lunar South Pole: Maximum Bolometric Temperatures and Permanently Shadowed Region Mapping," 44th Lunar and Planetary Science Conference, The Woodlands, TX, 2013. URL: https://www.lpi.usra.edu/meetings/lpsc2013/eposter/2617.pdf

[3] Sahinoz, A., "Landing Gear Design and Stability Evaluation of a Lunar Lander for Soft Landing," AIAA SPACE 2012 Conference, Pasadena, CA, Sept. 2012.

[4] Gibson, L. J., and Ashby, M. F., *Cellular Solids: Structure and Properties*, 2nd ed., Cambridge University Press, Cambridge, UK, 1997.

[5] Wei, H., Li, Y., and Zhao, B., "Research on Aluminum Honeycomb Buffer Device for Soft Landing on the Lunar Surface," *International Journal of Aerospace Engineering*, Vol. 2021, 2021, pp. 1–14. doi: 10.1155/2021/7686460

[6] Al-Ketan, O., and Abu Al-Rub, R. K., "Multifunctional Mechanical Metamaterials Based on Triply Periodic Minimal Surface Lattices," *Advanced Engineering Materials*, Vol. 21, No. 10, 2019, p. 1900524. doi: 10.1002/adem.201900524

[7] Feng, G., Li, S., Xiao, L., and Song, W., "Mechanical Properties and Deformation Behavior of Functionally Graded TPMS Structures Under Static and Dynamic Loading," *International Journal of Impact Engineering*, Vol. 176, 2023, p. 104554. doi: 10.1016/j.ijimpeng.2023.104554

[8] Al-Ketan, O., Rowshan, R., and Abu Al-Rub, R. K., "Topology-Mechanical Property Relationship of 3D Printed Strut, Skeletal, and Sheet Based Periodic Metallic Cellular Materials," *Additive Manufacturing*, Vol. 19, 2018, pp. 167–183. doi: 10.1016/j.addma.2017.12.006

[9] Paik, J. K., Thayamballi, A. K., and Kim, G. S., "The Strength Characteristics of Aluminum Honeycomb Sandwich Panels," *Thin-Walled Structures*, Vol. 35, No. 3, 1999, pp. 205–231. doi: 10.1016/S0263-8231(99)00026-9

[10] Kuenzi, E. W., "Mechanical Properties of Aluminum Honeycomb Cores," U.S. Forest Service, Research Note No. 1849, Madison, WI, Sept. 1955. URL: https://ir.library.oregonstate.edu/downloads/6108vg04p

[11] Lerch, B. A., "Properties of 5052 Aluminum for Use as Honeycomb Core in Manned Spaceflight," NASA Technical Memorandum NASA/TM-2018-219788, Glenn Research Center, Cleveland, OH, March 2018. URL: https://ntrs.nasa.gov/api/citations/20180001568/downloads/20180001568.pdf

[12] Arquilla, G., Ceci, A., Costanza, G., and Tata, M. E., "Effect of the Load Application Angle on the Compressive Behavior of Al Honeycomb under Combined Normal-Shear Stress," *Materials*, Vol. 16, No. 15, 2023, p. 5462. doi: 10.3390/ma16155462

[13] Kumar, R., Kumar, M., and Chohan, J. S., "The Role of Additive Manufacturing for Biomedical Applications: A Critical Review," *Journal of Manufacturing Processes*, Vol. 64, 2021, pp. 828–850. doi: 10.1016/j.jmapro.2021.02.022

[14] Abdulhadi, H., and Mian, A., "Developing Scaling Laws to Predict Compressive Mechanical Properties and Determine Geometrical Parameters of Modified BCC Lattice Structures," *Engineering Reports*, Vol. 4, No. 9, 2022, p. e12566. doi: 10.1002/eng2.12566

[15] Shi, W., Lin, Y., Li, J., Yang, M., and Liu, B., "Optimization of Mechanical Properties of Ti–6Al–4V Triply Periodic Minimal Surface Porous Structures Prepared by Laser Beam Powder Bed Fusion Technology Based on Orientation Control," *Journal of Materials Science and Technology*, Vol. 185, 2024, pp. 38–52. doi: 10.1016/j.jmst.2023.10.060

[16] Sun, Q., Sun, J., Guo, K., and Wang, L., "Investigation on Mechanical Properties and Energy Absorption Capabilities of AlSi10Mg Triply Periodic Minimal Surface Sheet Structures Fabricated via Selective Laser Melting," *Journal of Materials Engineering and Performance*, Vol. 31, 2022, pp. 9110–9121. doi: 10.1007/s11665-022-06883-5

[17] Shi, W., Lin, Y., Li, J., Yang, M., and Liu, B., "Study on the Energy Absorption Performance of Triply Periodic Minimal Surface (TPMS) Structures at Different Load-Bearing Angles," *Biomimetics*, Vol. 9, No. 7, 2024, p. 392. doi: 10.3390/biomimetics9070392

[18] Ntintakis, I., and Stavroulakis, G. E., "Mechanical and FEA-Assisted Characterization of Fused Filament Fabricated Triply Periodic Minimal Surface Structures," *Journal of Composites Science*, Vol. 5, No. 2, 2021, p. 58. doi: 10.3390/jcs5020058

[19] Novak, N., Al-Ketan, O., Krstulović-Opara, L., Rowshan, R., Abu Al-Rub, R. K., Vesenjak, M., and Ren, Z., "Quasi-Static and Dynamic Compressive Behaviour of Sheet TPMS Cellular Structures," *Composite Structures*, Vol. 266, 2021, p. 113801. doi: 10.1016/j.compstruct.2021.113801

[20] Arefin, A., Alam, M., and Gu, X., "Surface Morphology, Compressive Behavior, and Energy Absorption of Graded Triply Periodic Minimal Surface 316L Steel Cellular Structures Fabricated by Laser Powder Bed Fusion," *Materials*, Vol. 15, No. 23, 2022, p. 8528. doi: 10.3390/ma15238528